Electronic Supplementary Material (ESI) for Physical Chemistry Chemical Physics.

Supporting Information

Surface Chemical Trapping of Optical Cycling Centers

Han Guo[1], Claire E Dickerson[1], Ashley J. Shin[1], Changling Zhao[2], Timothy L. Atallah[1], Justin R. Caram[1], Wesley C. Campbell[2]*, Anastassia N. Alexandrova1**

[1] Department of Chemistry and Biochemistry, [2] Department of Physics and Astronomy, University of California, Los Angeles, Los Angeles, CA 90095, USA

Corresponding Author

Corresponding Authors' emails: jcaram@chem.ucla.edu, wes@physics.ucla.edu, ana@chem.ucla.edu

The electronic structure of SrOH in the gas phase was studied first using MRCI/state-average CASSCF with the def2-TZVPPD basis set[1–3] in Molpro.[4–9] Both the ground and the first excited states of SrOH were optimized using the state-average CASSCF (SA-CASSCF) with 9 electrons and 10 orbitals (9, 10) in the active space. We also tested for larger active spaces with more electrons or orbitals. The excitation energy difference between using the larger active spaces and the selected active space is less than 0.01 eV, and the difference in the Sr-O bond length change is less than 0.002 Å. The SA-CASSCF calculations are averaged over the ground state and the doubly degenerate excited state with a weight of 0.8/0.1/0,1 for the ground state calculation and a weight of 0.2/0.4/0.4 for the excited state calculation. The MRCI method with three reference states was used to compute the vertical excitation energies. Different weights were tested for both ground and excited states. The selected weights give the best performance in terms of the SCF convergence, and as compared to the experiment for the excitation energy. The results were then used to benchmark the performance of the Density Functional Theory (DFT) and TD-DFT methods. [10–13] The results are shown in Table S1 and S2.

Table S1. Comparison between different computational methods for ground state Sr-O bond length (r_{Sr-O}^{gs}), excited state Sr-O bond length (r_{Sr-O}^{ex}), Sr-O bond length change ($\Delta r_{Sr-O} = r_{Sr-O}^{ex} - r_{Sr-O}^{gs}$), and vertical excitation energy (ΔE) for SrOH excited from the electronic ground state to the first excited state. Results are compared to the band origins from experiments. For TD-DFT and CASSCF/MRCI calculations, the def2-TZVPPD basis set was used.

Method	r_{Sr-O}^{gs} (Å)	r_{Sr-O}^{ex} (Å)	Δr_{Sr-O} (Å)	ΔE (eV)
TD-DFT	2.095	2.073	-0.022	1.737
CASSCF/MRCI	2.145	2.117	-0.028	1.713
Experiments	2.111[14]	2.091[14]	-0.020	1.803, 1.836[15]

Table S2. Comparison between different basis sets and TD-DFT functionals for ground state Sr-O bond length (r^{gs}_{Sr-O}), excited state Sr-O bond length (r^{ex}_{Sr-O}), Sr-O bond length change (Δr_{Sr-O}), and vertical excitation energy (ΔE) for SrOH excited from the ground state to the first excited state. Results are compared to the band origins from experiments.

Functional	Basis set	r^{gs}_{Sr-O} (Å)	r^{ex}_{Sr-O} (Å)	Δr_{Sr-O} (Å)	ΔE (eV)
B3LYP-D3	def2-TZVPPD	2.115	2.096	-0.019	1.896
m062x	def2-TZVPPD	2.108	2.102	-0.006	2.228
wB97XD	def2-TZVPPD	2.113	2.087	-0.026	1.668
PBE0-D3	def2-TZVPPD	2.095	2.073	-0.022	1.737
PBE0-D3	def2-SVPD/ def2-TZVPPD	2.138	2.121	-0.017	1.750
Experiments		2.111[14]	2.091[14]	-0.020	1.803, 1.836[15]

Table S3. Comparison between computed vertical excitation energy (ΔE^{vert}), computed adiabatic excitation energy (ΔE^{ad}) and available experimental band origin (T_e) for SrOR excited from the ground state to the first excited state.[15]

Molecule	ΔE^{vert} (eV)	ΔE^{ad} (eV)	$T_e[A^2\Pi_{1/2}]$ (eV)	$T_e[A^2\Pi_{3/2}]$ (eV)
SrOH	1.750	1.736	1.803	1.836
$SrOCH_3$	1.754	1.739	1.800	1.835
$SrOC_4H_9$	1.738	1.723	1.795	1.829
$SrOC_{13}H_{21}$	1.721	1.702		

Table S4. Franck Condon Factors (FCFs) for the decay transitions from the ground state to the first excited state. The off-diagonal FCFs larger than 0.01 are also shown.

Molecules	Transition	FCF	Normal mode character
SrOH	0_0^0	0.9651	
	1_1^0	0.0341	Sr-O stretching
$SrOCH_3$	0_0^0	0.9556	
	1_1^0	0.0368	Sr-O stretching
$SrOC_4H_9$	0_0^0	0.9163	
	1_1^0	0.0555	Sr-O stretching
$SrOC_{13}H_{21}$	0_0^0	0.7819	
	1_1^0	0.1291	Sr-O stretching
	1_2^0	0.0110	Sr-O stretching
	2_2^0	0.0277	Sr-O-C bending

Table S5. Dipole electric fields applied along the Sr-O bond length (z-axis) direction for 1/32 ML Sr-O OCCs on a diamond surface. Electric field effects on atomic charges and Sr-O ground state bond lengths (r^{gs}_{Sr1-O}) are reported. Relaxation and single point calculations were performed with Perdew-Burke-Ernzerhof (PBE) functional and projector augmented-wave (PAW) potentials. Charges were computed via Bader Charge Analysis.

Field (V/m)	Sr-O charge	r^{gs}_{Sr-O} (Å)
-5.5 x 10^9	1.205 (Sr), -1.079 (O)	2.125
-1 x 10^9	0.9547 (Sr), -1.069 (O)	2.125
-1 x 10^8	0.9323 (Sr), -1.079 (O)	2.125
None	0.9391 (Sr), -1.079 (O)	2.125
1 x 10^8	0.9237 (Sr), -1.106 (O)	2.125
1 x 10^9	0.9156 (Sr), -1.080 (O)	2.120
5.5 x 10^{10}	0.4673 (Sr), -1.087 (O)	2.166

Table S6. Dipole electric fields applied along the Sr-O bond length (z-axis) direction for two SrO OCCs on a diamond surface spaced 3.88 Å apart, with 10.39 Å to the nearest other two OCCs. Electric field effects on atomic charges and Sr-O ground state bond lengths (r^{gs}_{Sr1-O}, r^{gs}_{Sr2-O}) are reported. Relaxation and single point calculations were performed with Perdew-Burke-Ernzerhof (PBE) functional and projector augmented-wave (PAW) potentials. Charges were computed via Bader Charge Analysis.

Field (V/m)	Sr1-O charges	Sr2-O charges	r^{gs}_{Sr1-O} (Å)	r^{gs}_{Sr2-O} (Å)
None	0.8447 (Sr) -1.065 (O)	0.9130 (Sr) -1.066 (O)	2.127	2.133
1 x 10^8	0.8031 (Sr) -1.055 (O)	0.8575 (Sr) -1.065 (O)	2.127	2.133
1 x 10^9	0.7832 (Sr) -1.056 (O)	0.8455 (Sr) -1.064 (O)	2.127	2.133
1 x 10^{10}	0.4642 (Sr) -1.114 (O)	0.4467 (Sr) -1.108 (O)	2.155	2.152

Table S7. Dipole electric fields applied along the Sr-O bond length (z-axis) direction and their effect on atomic charges, ground state Sr-O bond length (r^{gs}_{Sr-O}), excited state Sr-O bond length (r^{ex}_{Sr-O}) and bond length change (Δr^{gs}_{Sr-O}) for $SrOCH_3$. Calculations were performed at PBE0/def2-TZVPPD level of theory. Charges were computed via Natural Bond Order (NBO) analysis.

Field (V/m)	Ground state Sr-O charges	Excited state Sr-O charges	r^{gs}_{Sr-O} (Å)	r^{ex}_{Sr-O} (Å)	Δr^{gs}_{Sr-O} (Å)
-5.14 x 10^9	0.9531 (Sr) -1.204 (O)	0.9531 (Sr) -1.205 (O)	2.09202	2.07398	0.01804
-5.14 x 10^8	0.9612 (Sr) -1.167 (O)	0.9604 (Sr) -1.169 (O)	2.13724	2.11472	0.01802
-5.14 x 10^7	0.9609 (Sr) -1.162 (O)	0.9600 (Sr) -1.163 (O)	2.13679	2.11902	0.01777
None	0.9608 (Sr) -1.161 (O)	0.9598 (Sr) -1.163 (O)	2.137	2.119	0.018
5.14 x 10^7	0.9584 (Sr) -1.163 (O)	0.9568 (Sr) -1.164 (O)	2.09727	2.07576	0.02151
5.14 x 10^8	0.9571 (Sr) -1.157 (O)	0.9554 (Sr) -1.159 (O)	2.10148	2.07969	0.02179
5.14 x 10^9	0.9491 (Sr) -1.104 (O)	0.9521 (Sr) -1.102 (O)	2.14558	2.17948	0.03390

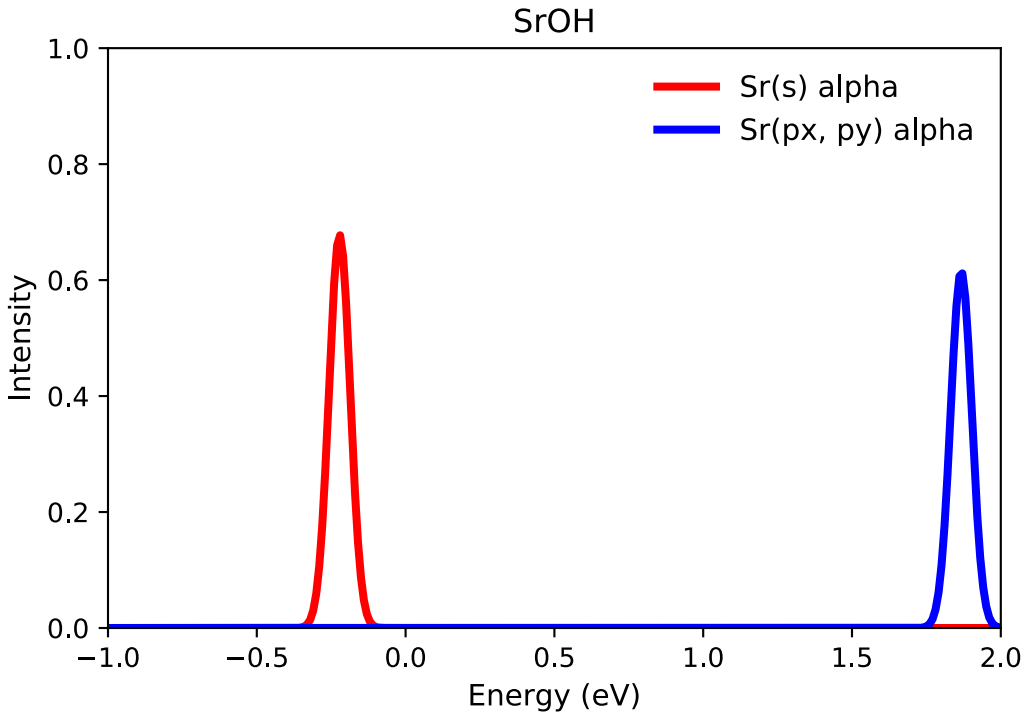

Figure S1. PDOS for SrOH molecule, indicating the excitation energy distance. Calculations were performed at HSE06 level of theory.

REFERENCES

(1) Pritchard, B. P.; Altarawy, D.; Didier, B.; Gibson, T. D.; Windus, T. L. *J. Chem. Inf. Model.* **2019**, *59* (11), 4814–4820.

(2) Weigend, F. *Phys. Chem. Chem. Phys.* **2006**, *8* (9), 1057–1065.

(3) Weigend, F.; Ahlrichs, R. *Phys. Chem. Chem. Phys.* **2005**, *7* (18), 3297–3305.

(4) Werner, H. J.; Knowles, P. J.; Knizia, G.; Manby, F. R.; Schütz, M. *Wiley Interdiscip. Rev. Comput. Mol. Sci.* **2012**, *2* (2), 242–253.

(5) Knowles, P. J.; Werner, H. J. *Theor. Chim. Acta* **1992**, *84*, 95–103.

(6) Knowles, P. J.; Werner, H. J. *Chem. Phys. Lett.* **1988**, *145* (6), 514–522.

(7) Werner, H. J.; Knowles, P. J. *J. Chem. Phys.* **1988**, *89* (9), 5803–5814.

(8) Werner, H. J.; Knowles, P. J. *J. Chem. Phys.* **1985**, *82* (11), 5053–5063.

(9) Werner, H.-J.; Knowles, P. J.; Knizia, G.; Manby, F. R.; Schütz, M.; Celani, P.; Györffy, W.; Kats, D.; Korona, T.; Lindh, R.; Mitrushenkov, A.; Rauhut, G.; Shamasundar, K. R.; Adler, T. B.; Amos, R. D.; Bennie, S. J.; Bernhardsson, A.; Berning, A.; Cooper, D. L.; Deegan, M. J. O.; Dobbyn, A. J.; Eckert, F.; Goll, E.; Hampel, C.; Hesselmann, A.; Hetzer, G.; Hrenar, T.; Jansen, G.; Köppl, C.; Lee, S. J. R.; Liu, Y.; Lloyd, A. W.; Ma, Q.; Mata, R. A.; May, A. J.; McNicholas, S. J.; Meyer, W.; {Miller III}, T. F.; Mura, M. E.; Nicklaß, A.; O'Neill, D. P.; Palmieri, P.; Peng, D.; Pflüger, K.; Pitzer, R.; Reiher, M.; Shiozaki, T.; Stoll, H.; Stone, A. J.; Tarroni, R.; Thorsteinsson, T.; Wang, M.; Welborn, M. .

(10) Liu, J.; Liang, W. *J. Chem. Phys.* **2011**, *135* (18), 184111.

(11) Liu, J.; Liang, W. *J. Chem. Phys.* **2011**, *135* (1), 014113.

(12) Furche, F.; Ahlrichs, R. *J. Chem. Phys.* **2002**, *117* (16), 7433–7447.

(13) Bauernschmitt, R.; Ahlrichs, R. *Chem. Phys. Lett.* **1996**, *256*, 454–464.

(14) Yu, S.; Wang, J. G.; Sheridan, P. M.; Dick, M. J.; Bernath, P. F. *J. Mol. Spectrosc.* **2006**, *240* (1), 26–31.

(15) Brazier, C. R.; Ellingboe, L. C.; Kinsey-Nielsen, S.; Bernath, P. F. *J. Am. Chem. Soc.* **1986**, *108* (9), 2126–2132.